https://ntrs.nasa.gov/search.jsp?R=20190002540 2020-05-10T03:38:37+00:00Z



Environmental Research Letters

CrossMark

OPEN ACCESS

RECEIVED
2 January 2018

REVISED
26 April 2018

ACCEPTED FOR PUBLICATION
9 May 2018

PUBLISHED
7 June 2018

Original content from this work may be used under the terms of the Creative Commons Attribution 3.0 licence.

Any further distribution of this work must maintain attribution to the author(s) and the title of the work, journal citation and DOI.

LETTER

# Quantifying long-term changes in carbon stocks and forest structure from Amazon forest degradation

**Danielle I Rappaport[1,6], Douglas C Morton[2], Marcos Longo[3,4], Michael Keller[3,4,5], Ralph Dubayah[1] and Maiza Nara dos-Santos[3]**

[1] Department of Geographical Sciences, University of Maryland, College Park, MD, United States of America
[2] NASA Goddard Space Flight Center, Greenbelt, MD, United States of America
[3] Embrapa Agricultural Informatics, Brazilian Agricultural Research Corporation (EMBRAPA), Campinas, SP, Brazil
[4] NASA Jet Propulsion Laboratory, California Institute of Technology, Pasadena, CA, United States of America
[5] USDA Forest Service, International Institute of Tropical Forestry, San Juan, Puerto Rico
[6] Author to whom any correspondence should be addressed.

**E-mail:** drappap@umd.edu

**Keywords:** aboveground biomass, forest structure, habitat, understory fires, carbon cycling, airborne lidar, REDD+

Supplementary material for this article is available online

## Abstract

Despite sustained declines in Amazon deforestation, forest degradation from logging and fire continues to threaten carbon stocks, habitat, and biodiversity in frontier forests along the Amazon arc of deforestation. Limited data on the magnitude of carbon losses and rates of carbon recovery following forest degradation have hindered carbon accounting efforts and contributed to incomplete national reporting to reduce emissions from deforestation and forest degradation (REDD+). We combined annual time series of Landsat imagery and high-density airborne lidar data to characterize the variability, magnitude, and persistence of Amazon forest degradation impacts on aboveground carbon density (ACD) and canopy structure. On average, degraded forests contained 45.1% of the carbon stocks in intact forests, and differences persisted even after 15 years of regrowth. In comparison to logging, understory fires resulted in the largest and longest-lasting differences in ACD. Heterogeneity in burned forest structure varied by fire severity and frequency. Forests with a history of one, two, and three or more fires retained only 54.4%, 25.2%, and 7.6% of intact ACD, respectively, when measured after a year of regrowth. Unlike the additive impact of successive fires, selective logging before burning did not explain additional variability in modeled ACD loss and recovery of burned forests. Airborne lidar also provides quantitative measures of habitat structure that can aid the estimation of co-benefits of avoided degradation. Notably, forest carbon stocks recovered faster than attributes of canopy structure that are critical for biodiversity in tropical forests, including the abundance of tall trees. We provide the first comprehensive look-up table of emissions factors for specific degradation pathways at standard reporting intervals in the Amazon. Estimated carbon loss and recovery trajectories provide an important foundation for assessing the long-term contributions from forest degradation to regional carbon cycling and advance our understanding of the current state of frontier forests.

## Introduction

Changes in Amazon forest carbon stocks are a significant source of greenhouse gas emissions from human activity (van der Werf *et al* 2009, Pan *et al* 2011, Aguiar *et al* 2016). Understanding the long-term response of Amazon forests to land use and climate is essential for balancing the global carbon budget and improving climate projections (e.g. Gatti *et al* 2014, Friedlingstein *et al* 2014). Although annual deforestation rates in the Brazilian Amazon have declined by 80% since 2004 (Hansen *et al* 2014, INPE 2015), forest degradation from fire and logging remains a threat to forest carbon stocks across the Amazon *arc of deforestation* (Morton *et al* 2013). The magnitude of carbon losses from forest degradation is large (Longo *et al* 2016),

© 2018 The Author(s). Published by IOP Publishing Ltd

but the long-term consequences of fire and logging on forest structure and composition remain uncertain (Andrade *et al* 2017).

Decades of Amazon frontier expansion have left a mosaic of degraded forests along the Amazon arc of deforestation (Asner *et al* 2005, Morton *et al* 2013). Nearly 3% of southern Amazonia burned between 1999–2010, and the persistence of burned frontier forests (Morton *et al* 2013) underscores the importance of considering fire separately from deforestation for complete forest carbon accounting. Selective logging is also widespread across the leading edge of frontier expansion. In 2009 alone, 14.2 million $m^3$ of round wood was extracted from the largest logging centers in the Brazilian Legal Amazon (Pereira *et al* 2010). Canopy damage in logged forests can increase vulnerability to additional disturbances, including fire (Uhl and Vieira 1989, Holdsworth and Uhl 1997), but the feedbacks and synergies among disturbance agents, as well as the long-term impacts of degradation, are still largely unresolved.

The scarcity of large-scale, long-term studies on fire and logging impacts has undermined efforts to quantify emissions from Amazon forest degradation for global carbon accounting (Le Queré *et al* 2016) and climate mitigation efforts (Andrade *et al* 2017). Reducing land-use emissions is one cost-effective climate mitigation pathway (e.g. Canadell and Raupach 2008, Griscom *et al* 2017), including efforts to reduce emissions from deforestation and forest degradation (REDD+) under the United Nations Framework Convention on Climate Change. To be eligible for REDD+ performance-based payments, countries must be able to monitor, report, and verify (MRV) reductions in carbon emissions from degradation or deforestation. However, because of large uncertainties regarding net carbon emissions from fire and logging, degradation has remained poorly integrated within the REDD+ accounting framework (Mertz *et al* 2012, Goetz *et al* 2015) and excluded from national reporting (e.g. Brazil 2014).

The challenge to quantify degradation emissions stems from the heterogeneity and time-dependence of degradation impacts (Longo *et al* 2016, Andrade *et al* 2017). The variability in degradation impacts may result from regional differences in underlying biomass distributions (Avitabile *et al* 2016, Longo *et al* 2016), forest resilience to fire (Brando *et al* 2012, Flores *et al* 2017), and land use (Aragão and Shimabukuro 2010). Discrepancies in emissions estimates also stem from methodological differences among studies. Field-based studies provide valuable context for understanding the long-term impacts of degradation (e.g. Berenguer *et al* 2014), but forest inventory measurements typically have limited spatial and temporal coverage due to cost constraints. By contrast, experimental studies control for much of the variability in degradation history but may be limited in their capacity to simulate the diversity of degradation impacts (e.g. Brando *et al* 2014). Consequently, existing estimates for committed carbon emissions from Amazon understory fires vary by an order of magnitude, ranging from ~20 Mg C $ha^{-1}$ (Brando *et al* 2014) to 263 Mg C $ha^{-1}$ (Alencar *et al* 2006). Airborne lidar provides the spatially extensive and structurally detailed information on forest structure and aboveground carbon stocks needed to reconcile previous estimates of degradation emissions and quantify co-benefits of avoided degradation (Goetz *et al* 2015, Longo *et al* 2016, Sato *et al* 2016).

Here, we used a purposeful sample of high-density airborne lidar to capture a broad range of degraded and intact forest conditions in the southern Brazilian Amazon. For each forest stand, we combined degradation history information from annual time series of Landsat data with airborne lidar data to characterize canopy structure and estimate aboveground carbon density (ACD) using a lidar-biomass model specifically developed for frontier forests in the Brazilian Amazon (Longo *et al* 2016). Our large-area lidar coverage and sampling chronosequence addressed two questions: (1) What are the trajectories of loss and recovery of forest carbon stocks and habitat structure following fire and logging in frontier Amazon forests? (2) How do degradation type, frequency, and severity contribute to variability in degraded forest carbon stocks and habitat structure over time? Our study directly targets a lingering data gap for REDD+ (Andrade *et al* 2017) by quantifying the rates of ACD recovery over 1- to 15-year time horizons following a broad range of degradation pathways, including sequential impacts of logging and burning. These time-varying emissions estimates, or emissions factors, can be combined with activity data on the extent of forest degradation to establish REDD+ baselines; confirm the relative contributions from fire, logging, and regeneration to regional net forest carbon emissions; and estimate the consequences to mitigation targets if degradation remains omitted from greenhouse gas accounting. Airborne lidar also provides detailed, quantitative information on habitat structure that may support an improved understanding of the biodiversity co-benefits of reducing forest degradation—an integral, but poorly formalized component of REDD+ MRV.

## Methods

### Study area

The study area covers approximately 20 000 $km^2$ at the southern extent of closed-canopy Amazon forests in the Brazilian state of Mato Grosso (figure 1). Mean annual precipitation (1895 mm) and temperature (25 °C) support tropical forests and a diversity of land uses (Souza *et al* 2013). A four-month dry season (figure S1 available at stacks.iop.org/ERL/13/065013/mmedia) and periodic drought events (Chen *et al* 2011) contribute to the extent, duration, and severity of understory forest fires in the study region

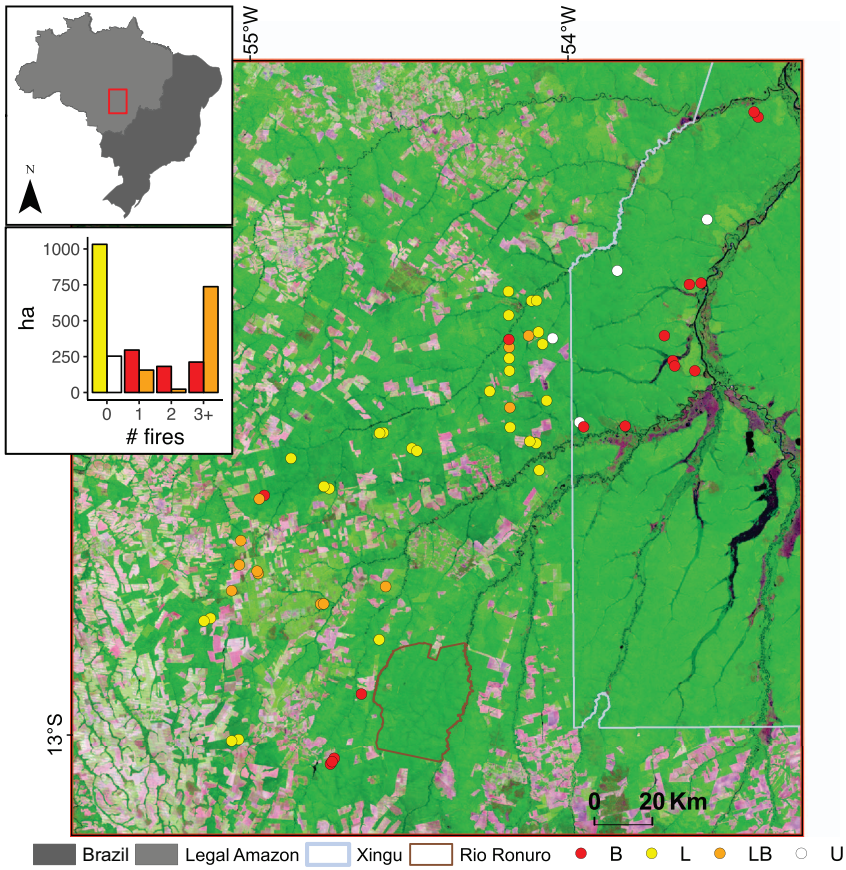


**Figure 1.** Degraded and intact forest stands were distributed across 20 000 km$^2$ in the Brazilian state of Mato Grosso (top inset). In the false-color composite image (2014 Landsat, bands 543), forest appears green, deforested areas appear pink, and wetland and open water appear purple. Circles indicating the centroid of forest stands with lidar coverage are color-coded by degradation history (U—undisturbed; L—logged; LB—logged and burned; B—burned). Airborne lidar data sampled frontier forests on private lands and within the Xingu Indigenous Park (light blue outline) and along a degradation gradient (bottom inset).

(Morton *et al* 2013, Brando *et al* 2014). Additionally, decades of agricultural expansion and selective logging (e.g. Asner *et al* 2005, Souza *et al* 2005, Matricardi *et al* 2007) have left a patchwork of fragmented and degraded forests in the study area, with few intact forests remaining outside of the Xingu Indigenous Reserve or Rio Ronuro Ecological Station (figure 1).

## Data and analysis

We combined Landsat time series and airborne lidar data to quantify variability in forest structure and ACD across gradients of degradation type, frequency, severity, and timing. Degradation history for areas with lidar coverage was characterized using a two-tiered classification approach. First, the annual occurrence of logging, understory fires, and deforestation was mapped based on spatial, spectral, and temporal information derived from annual time series of cloud-free Landsat mosaics for the early dry season months (June–August) of 1984–2016 (figure S2; text S1). Understory fires and deforestation events were identified based on multi-year patterns of damage and recovery in Landsat Normalized Difference Vegetation Index (NDVI) (Morton *et al* 2011, Morton *et al* 2013). Logged forests were identified with an automated detection approach based on the spatial distribution of log landing decks (Asner *et al* 2004, Keller *et al* 2004). Mutually exclusive classification rules for the magnitude, duration, size, and shape of deforestation and degradation events avoided double counting errors common with the integration of independent products (figure S2; text S1) (Morton *et al* 2011, Bustamante *et al* 2016). Second, forest stands of uniform degradation history were manually delineated within the extent of lidar coverage and visually validated to confirm the extent and timing of degradation events. Logging roads visible in multiple years of Landsat data were excluded from logged forest stands to control for the impact of logging infrastructure on estimated carbon stocks and recovery trajectories.

Airborne lidar data were used to estimate ACD in intact and degraded forest types stratified by degradation history. High-density airborne lidar data (minimum of 14 returns per m$^2$) were collected as part of the Sustainable Landscapes Brazil project across a range of intact and degraded forests in a space-for-time substitution sampling design (table S1, data available from: www.paisagenslidar.cnptia.embrapa.br/webgis/). Based on the classification

approach described above, the 2891.25 ha of lidar coverage were stratified into 58 forest stands (4.50–498.50 ha; table S2).

A lidar-biomass model based on mean top of canopy height (TCH, m) (Longo *et al* 2016) was used to estimate ACD (kg C $m^{-2}$) in forest stands at 0.25 ha resolution:

$$ACD_{TCH} = 0.054\,(\pm 0.012)\,TCH^{1.76(\pm 0.07)} \quad (1)$$

where the parenthetical values are the standard errors of the parameters. Equation (1) assumes a biomass-to-carbon conversion factor of 0.5, following Baccini *et al* (2012). We selected the TCH model because of its simplicity, sensitivity to the lower range of the ACD distribution, and accurate representation of ACD in burned forests (Longo *et al* 2016). Equation (1) was developed using inventory and lidar data from intact and degraded Amazon forests. Here, we applied the model to a new set of lidar data sampled from the same regional context in which the Longo *et al* (2016) model was calibrated; about 8% of the lidar data set overlapped with the data used in model development.

Pixel-based uncertainty associated with modeled ACD was calculated from three sources of statistical uncertainty following the methods described in Longo *et al* (2016). A Monte Carlo approach with 10 000 iterations was used to propagate the pixel-based uncertainty to the stand level by adjusting each biomass pixel with randomly distributed noise proportionate to its uncertainty before aggregating data at the stand level. The stand-level standard error was derived from the standard deviation of the simulated stand-level means.

Given the importance of canopy structure for wildlife habitat in tropical forests (Bergen *et al* 2009), we also calculated two lidar-based measures of habitat structure. First, residual canopy cover was calculated using 1 m resolution lidar canopy height models (CHMs) as the proportion of the forest stand greater than or equal to the mean canopy height in intact forests (21 m). Second, clusters of one or more canopy trees (≥21 m) were identified using the 1 m CHMs with a maximum search radius of 10 m using a 3 × 3 pixel moving window (Silva *et al* 2015). These metrics provided complementary information on changes in forest structure from degradation and recovery processes to assess the drivers of ACD variability and the time-varying recovery of both carbon and habitat structure in degraded forests.

We used multiple linear regression to model the loss and recovery trajectories of ACD and canopy structure based on the chronosequence of lidar samples. Four least squares models were fit using the lm function in R version 3.3.0 (www.R-project.org). Model 1 estimated median ACD in degraded forest stands based on degradation type (burned or logged-only), timing (years since last degradation event), and fire frequency. Median ACD was selected as the measure of central tendency for each stand because of the skewed ACD distributions in degraded forests. Model 2 further stratified once-burned forests by fire severity, visible as rings of high- and low-severity canopy damage, based on the relative difference between the pre-fire and post-fire Landsat dry-season NDVI (RdNDVI). A fixed threshold of mean minus the standard deviation of RdNDVI was only used to stratify low and high-severity fire damages in once-burned stands because the spatial variability of fire damages was not well preserved following recurrent fire events. Models 3 and 4 used degradation type, timing, and frequency to predict residual canopy cover and density of canopy tree clusters, respectively. In all four models, the variable for time since last degradation event was log-transformed to satisfy assumptions of normality and homoscedasticity (Vargas *et al* 2008, Becknell *et al* 2012). Additionally, to isolate the effect of forest recovery from the long-term impacts of logging infrastructure, logged forest stands were adjusted to exclude secondary roads and log landing decks. Interactions between degradation history (type, frequency, severity) and degradation timing were evaluated for significance and model performance in all four models. Lastly, differences across degradation strata were evaluated using pairwise Wilcoxon tests to accommodate the diversity of non-normal data distributions.

Consistent with recommendations from the Intergovernmental Panel on Climate Change (Penman *et al* 2003), an additional Monte Carlo procedure was used to propagate the effect of ACD uncertainty on model parameters and predictions by performing 10 000 realizations of the model fit on adjusted stand-level medians with normally distributed noise proportional to the stand-level standard error, or the standard deviation of the stand-level Monte Carlo aggregations.

## Results

Degradation type, frequency, timing, and severity contributed to ACD variability in frontier forests. Lidar-based estimates of ACD in 58 Amazon forest stands varied by nearly two orders of magnitude between the most heavily degraded forest stand (median: 4.5 Mg C $ha^{-1}$), a stand that had been logged and burned three times, and the most carbon-dense intact forest stand (median: 114.3 Mg C $ha^{-1}$; table S2). At the pixel scale, median carbon density in degraded forests (51.2 Mg C $ha^{-1}$) was less than half of ACD in intact forests (113.5 Mg C $ha^{-1}$). Degraded ACD was also more heterogeneous than intact ACD (coefficient of variation: 68.4% and 16.7% for degraded (2638.00 ha) and intact forest pixels (253.25 ha), respectively).

The variability in ACD following degradation could not be constrained by degradation type alone. ACD in pixels with a history of fire (median: 20.4 Mg C $ha^{-1}$;

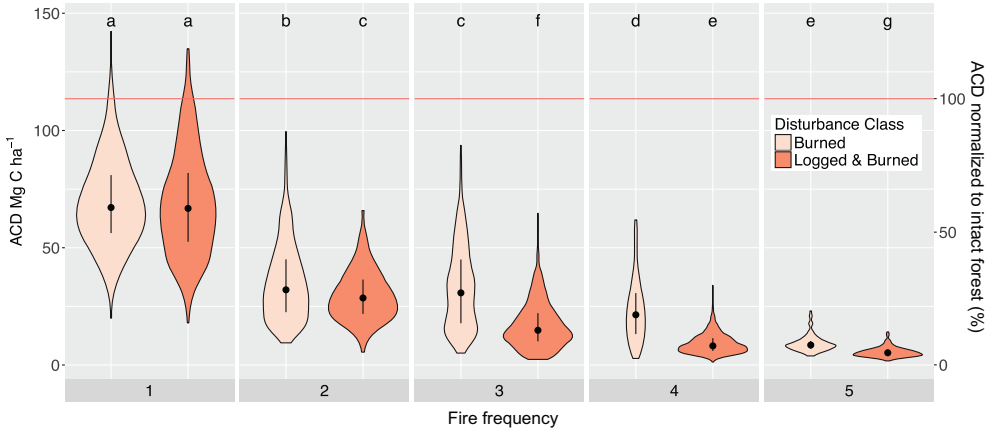


**Figure 2.** Forests affected by multiple fires had the largest differences in aboveground carbon density (ACD) compared to median ACD in intact forests (red line). Additionally, ACD distributions between burned and logged-and-burned forests were similar for once-burned forests. The violin plots summarize ACD distributions as a function of fire frequency and degradation class. The median and interquartile range of each group are indicated with the black circle and line. The tails of the violins are trimmed to the range of data, and all violins have the same area prior to trimming the tails. Distinct letters indicate significant differences among distributions from a pairwise Wilcoxon test with a Holm correction procedure to adjust $\alpha$ for multiple testing. See figure S4(*a*) for a comparison across burn frequency groups that also accounts for stand age.

1605.75 ha) was significantly lower ($p < 0.05$) than ACD in logged-only pixels (77.8 Mg C ha$^{-1}$; 1032.25 ha); however, ACD varied broadly within both degradation classes. At the stand level, there was considerable overlap between the ranges of median ACD in burned forests (4.5–95.2 Mg C ha$^{-1}$) and logged-only forests (39.0–117.3 Mg C ha$^{-1}$, table S2).

Degradation timing was a critical factor for further differentiating ACD between and within logged and burned forest classes (figure S3; table 1). Within two years of recovery, median ACD in burned pixels was 9.5 Mg C ha$^{-1}$, compared to 68.4 Mg C ha$^{-1}$ in logged-only pixels. Following 10 to 15 years of recovery, neither class recovered its estimated pre-disturbance ACD, and median ACD in burned pixels remained considerably lower than in logged pixels (difference: 17.5 Mg C ha$^{-1}$).

Fire frequency governed both the magnitude and the spatial pattern of residual forest carbon stocks (figures 2 and 3; table 1). Repeated burning resulted in a non-linear decline in ACD, irrespective of logging history, with lowest ACD in forests subjected to three or more fires (figure 2). Forests affected by a single fire ($n = 10$) retained 67.0 Mg C ha$^{-1}$ (interquartile range [IQR] $\pm$ 26.4 Mg C ha$^{-1}$). Twice-burned forests ($n = 5$) contained less than half the carbon stocks in once-burned forests (31.6 $\pm$ 21.1 Mg C ha$^{-1}$). Forests burned three to five times ($n = 13$) retained few trees from the pre-fire forest stand; ACD was only one-sixth of that of once-burned forests (10.3 Mg C ha$^{-1}$), with the narrowest IQR of all burn frequencies ($\pm$10.5 Mg C ha$^{-1}$). Importantly, the observed decrease in IQR with increasing fire frequency indicated a reduction in structural complexity from repeated burning (figures 2 and 3).

Unlike the impact of successive fires, there was no significant long-term impact on ACD recovery attributable to prior logging after controlling for fire frequency (figure S4). Because the distinction between burned and logged-and-burned forests was not a statistically significant predictor of degraded forest ACD, nor did it improve model fit, logged-and-burned and burned forest stands were combined to model post-fire recovery of ACD.

Fire frequency and the time since the last degradation event explained the greatest variability in degraded ACD recovery (Model 1; adjusted $R^2 = 0.89$; $F$-statistic = 106.5 figure 4(*a*); table S3). The immediate reduction in ACD differed significantly for each degradation pathway (regression intercept; table S3). In the year following degradation, the modeled ACD for forests that had been logged, once-burned, twice-burned, and subjected to three or more burns was 62.3, 52.0, 19.4, and 11.0 Mg C ha$^{-1}$, respectively. However, the rate of ACD recovery was similar for all classes, as interaction effects between fire frequency and time since degradation event were not statistically significant (table S3). Given these initial differences and the slow recovery in degraded forest ACD, the legacy of forest degradation was still evident 15 years following fire and logging (table 2).

Initial fire severity was a statistically significant predictor of ACD recovery in once-burned forests (Model 2; Adjusted $R^2 = 0.88$; $F$-statistic = 87.87; figure 4(*b*); tables 2 and S3). In the year following fire, estimated high- and low-severity damages differed by 16% of intact ACD (table 2). Modeled differences in ACD resulting from initial fire severity were preserved through time, with once-burned forests recovering between 57.6% and 73.9% of intact ACD after 15 years of recovery, depending on initial fire severity (figure 4(*b*); table 2). Covariation of ACD with Landsat and lidar metrics of canopy density in burned forests provided additional insights into the contribution of fire

**Table 1.** Forest degradation from logging and fire alters ACD and stand structure relative to neighboring intact forests. Lidar-based estimates of the fraction of original canopy cover, number of canopy tree clusters, and the distribution of ACD in degraded forests. Degraded forests were partitioned along three axes of variability—degradation type, frequency, and timing. The lower, middle (median) and upper quartile of aboveground biomass density (Mg C $ha^{-1}$) are shown as $ACD_{25}$, $ACD_{50}$, and $ACD_{75}$, respectively.

| | Intact | Logged (1–2 yrs) | Logged (4–5 yrs) | Logged (10–11 yrs) | Logged (14–15 yrs) | Logged (18–20 yrs) | Fire 1x (1–2 yrs) | Fire 1x (4–5 yrs) | Fire 1x (10–11 yrs) | Fire 1x (14–15 yrs) | Fire 2x | Fire 3x+ |
|---|---|---|---|---|---|---|---|---|---|---|---|---|
| % Original canopy | 100 | 46.9 | 60.1 | 61.6 | 76.7 | 83.3 | 21.7 | 47.0 | 58.5 | 58.4 | 20.1 | 5.3 |
| Num. canopy clusters | 170 | 79 | 104 | 111 | 127 | 145 | 34 | 78 | 92 | 99 | 31 | 8 |
| $ACD_{25}$ | 102.1 | 52.3 | 64.9 | 80.4 | 83.8 | 86.4 | 53.0 | 55.5 | 58.4 | 83.3 | 22.3 | 6.6 |
| $ACD_{50}$ | 113.5 | 68.4 | 76.8 | 89.7 | 98.8 | 105.5 | 64.3 | 65.6 | 74.0 | 91.0 | 31.6 | 10.3 |
| $ACD_{75}$ | 125.1 | 84.0 | 88.8 | 99.8 | 111.6 | 121.0 | 72.2 | 76.6 | 89.8 | 100.2 | 43.4 | 17.1 |

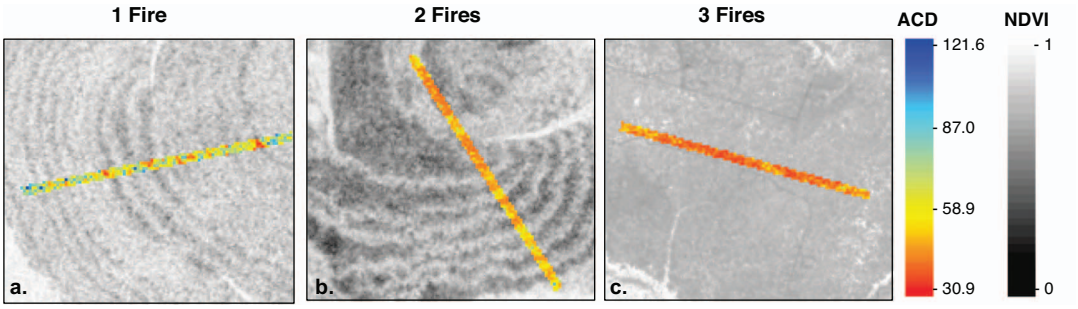


**Figure 3.** Ring patterns in burned forests indicate diurnal differences in fire line intensity, and increasing fire frequency results in a progressive loss of forest biomass and structural diversity. Lidar-based estimates of aboveground carbon density (ACD, Mg C ha$^{-1}$) at 0.25 hectare resolution for 5000 × 200 m transects are overlaid on post-fire Landsat NDVI for once-burned (*a*) twice-burned (*b*) and thrice-burned (*c*) forest stands. See tables S1 and S2 for additional profile information associated with each stand (stand IDs from left to right: 26, 13, and 8).

**Table 2.** Estimates based on the multiple linear regression models of aboveground carbon density predicted at four standard reporting periods following the most common logging and fire pathways. For each degradation class, modeled ACD and 95% confidence interval (in parentheses) are shown as the percentage of the intact forest reference (113.5 Mg C ha$^{-1}$). The confidence interval was calculated based on the mean of 10 000 confidence intervals generated from the Monte Carlo linear regressions, which were iteratively fit to the stand-level biomass estimates adjusted with noise proportionate to the stand-level standard errors. Model predictions for low- and high-severity fires are derived from model 2; all other predictions presented here are derived from model 1 (see table S3).

| | Logged | | Burned 1x (Average) | | Burned 1x (Low) | | Burned 1x (High) | | Burned 2x | | Burned 3x+ | |
|---|---|---|---|---|---|---|---|---|---|---|---|---|
| Y1 | 54.8 | (49.4–60.3) | 45.8 | (38.0–53.6) | 48.6 | (41.1–56.1) | 32.2 | (24.1–40.3) | 17.1 | (8.5–25.8) | 9.7 | (4.5–14.9) |
| Y5 | 71.0 | (67.5–74.5) | 61.9 | (56.3–67.6) | 63.6 | (58.0–69.3) | 47.3 | (41.0–53.6) | 33.3 | (25.2–41.4) | 25.8 | (20.0–31.7) |
| Y10 | 77.9 | (73.6–82.3) | 68.9 | (63.1–74.7) | 70.1 | (64.4–75.8) | 53.8 | (47.4–60.1) | – | – | – | – |
| Y15 | 82.0 | (76.9–87.1) | 73.0 | (66.8–79.1) | 73.9 | (67.9–80.0) | 57.6 | (51.0–64.2) | – | – | – | – |

severity to ACD variability within a single fire (figures S6 and S7).

Changes in canopy structure from logging and fire were also persistent after 15 years of forest recovery (figure S5; table 1). Degradation timing and fire frequency explained the greatest variability in the recovery trajectory of residual canopy (Model 3; adjusted $R^2 = 0.74$; F-statistic = 38.85) and density of canopy trees (Model 4; adjusted $R^2 = 0.76$; F-statistic = 36.3; figure S5; table S4). Understory fires resulted in the largest reduction of canopy tree clusters, particularly following recurrent fires. Logged forests retained more than twice as many canopy tree clusters (46.5%) as once-burned forests (20.0%) when measured within 1–2 years of the degradation event. Forests burned three or more times retained only 4.7% the number of canopy tree clusters found in intact forests. After 14–15 years of regrowth, once-burned forests recovered only 80% of the canopy tree clusters present in logged forests. Further, these impacts to forest structure may persist even after ACD in degraded forests returns to pre-degradation levels. For example, after 14–15 years of regrowth, once-burned forests recovered a larger fraction of intact-forest ACD (80.2%) than canopy tree clusters (58.2%).

## Discussion

Amazon forest degradation from logging and fire has a lasting impact on forest carbon stocks and canopy structure. The slow recovery of degraded forests underscores the need to address drivers of degradation to ensure the retention of carbon stocks and preserve complex canopy structure in frontier Amazon forests. Using a large sample of intact and degraded forests, we provide the first comprehensive look-up table of degradation emissions factors for Amazon forests to guide the incorporation of forest degradation within REDD+ MRV (tables 1 and 2). Our findings illustrate the persistence of degradation impacts beyond the time scales for REDD+ MRV and even REDD+ baselines (typically 10 years), providing the foundation for further investigations into the relative contributions from fire and logging to regional land-use emissions. ACD in degraded forests varied by two orders of magnitude across the study area (table S2), providing clear support for the creation of multiple classes of forest degradation within REDD+ or other carbon accounting frameworks based on degradation frequency, severity, and timing. Overall, understory fires led to larger and more persistent changes in ACD and forest structure than logging, consistent with previous findings from Longo *et al* (2016). Our results further demonstrate how fire severity and fire frequency contribute to non-linear declines in ACD and homogenization of degraded forest structure (figure 2, tables 1 and 2). Collectively, these results address key data gaps that have hindered MRV of Amazon forest degradation.

Lidar-based estimates of carbon losses from fire were much larger than previous reports from experimental studies and forest inventories. For example, the reduction in ACD one year following a single burn

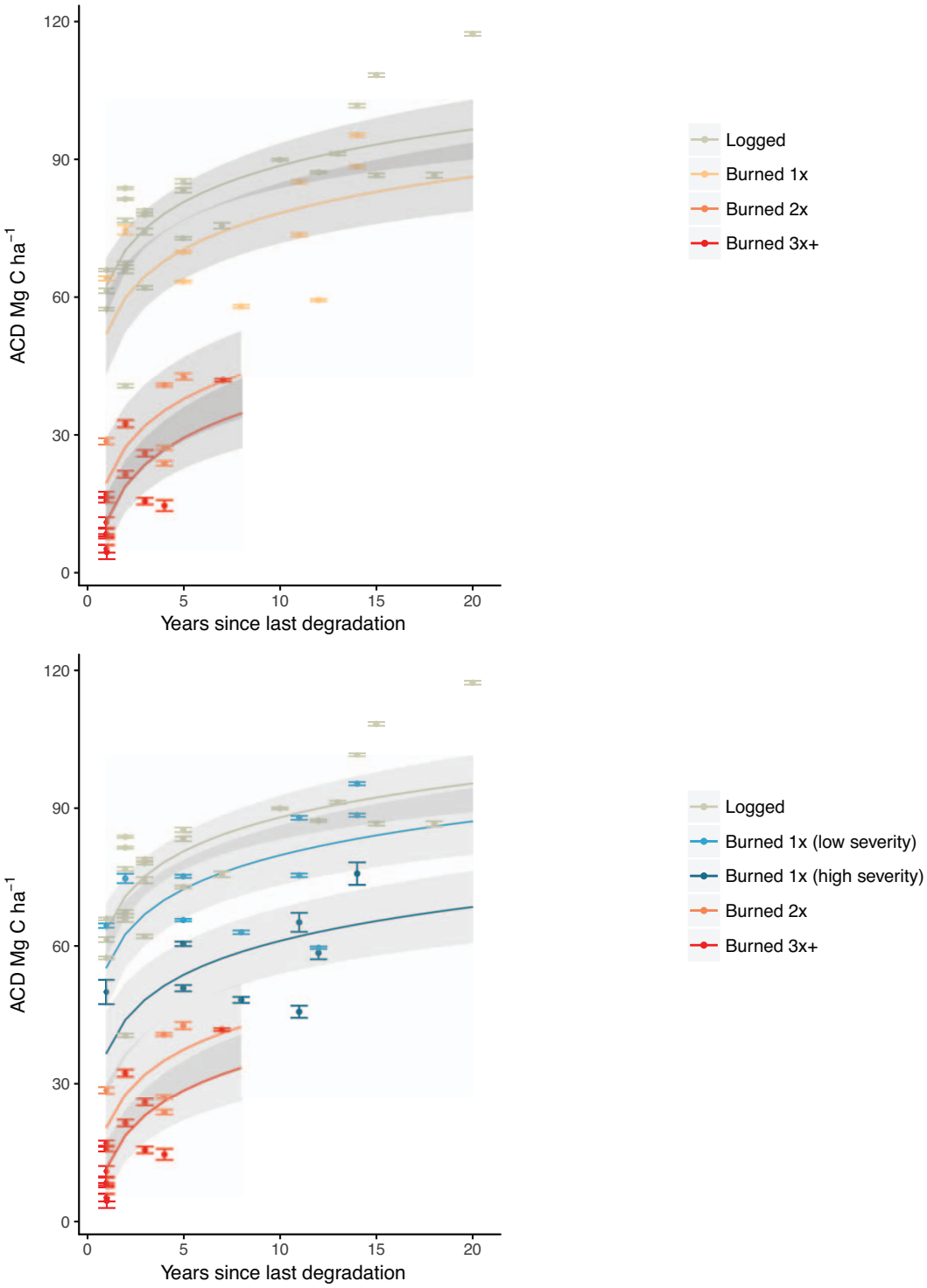


**Figure 4.** Patterns of aboveground biomass recovery following forest degradation highlight the magnitude and duration of ACD accumulation following fire. (*a*) Relationship between ACD and stand age for forests that were logged, burned once, burned twice, and burned three or more times. (*b*) Initial fire severity in once-burned forests further explains the heterogeneity in residual carbon stocks. Points correspond to estimated stand-level medians, error bars correspond to stand-level standard errors derived from 10 000 Monte Carlo stand-level aggregations, and the shaded bands represent the mean 95% confidence interval from 10 000 Monte Carlo simulations of the model fit. Model details are presented in table S3.

in this study (54.2%) was approximately three times larger than from experimental fires in the southeastern Amazon (Brando *et al* 2014). This discrepancy may reflect the improved capacity to characterize the heterogeneity of wildfire damages using airborne lidar or the difficulty for prescribed fires in experimental studies to replicate the emergent properties of wildfires, such as fire front intensity. Field studies have also reported smaller relative losses in ACD following fire (13.7%; Berenguer *et al* 2014). These differences may reflect the confounding influence of different age classes and burn frequencies, the challenges of

capturing the length scales of spatial variability (see figure 3) using typical inventory plots (0.25–1.0 ha), or regional variability in fire intensity from climatic and forest-type specific responses to fire (e.g. Flores *et al* 2017). These broad discrepancies reinforce the need for large-scale studies of additional frontier landscapes to support emissions mitigation programs, including REDD+ MRV.

Reducing the incidence and frequency of understory forest fires would preserve both carbon stocks and habitat structure in frontier landscapes. The marginal carbon cost of recurrent fire events in this study suggests that avoiding just one additional fire in a previously burned forest would retain carbon stocks equivalent to one-third of the intact reference ACD. Notably, not all degradation sequences have the same cumulative impact. We contrast the non-linear impact of recurrent burns with the effect of selective logging before fire. In the case of recurrent burns, each fire leads to a greater proportional loss. However, logging before fire did not amplify the long-term carbon losses from fire, after accounting for fire frequency; nor was logging a significant predictor of carbon recovery, regardless of fire history. These findings suggest that the distribution of fine litter (e.g. Balch *et al* 2008) may be a more important determinant of fire damage than large woody debris or canopy openings from logging.

The slow recovery of degraded ACD suggests that the continued omission of degradation from carbon accounting may result in substantial underreporting of forest carbon emissions. Relative to baseline periods, the frequency and severity of Amazon droughts (Boisier *et al* 2015, Duffy *et al* 2015) are projected to increase degradation risk in coming decades (Nobre *et al* 2016, Le Page *et al* 2017). The look-up table of proportional losses between degraded and intact forests developed in this study may facilitate the integration of carbon losses from fire and logging into REDD+ monitoring and reporting protocols. Further, accounting for carbon emissions from forest degradation may also reduce uncertainties in the Amazon carbon budget. Previous studies have either excluded a post-disturbance recovery term (Aragão *et al* 2014) or have combined secondary and degraded forests (Houghton *et al* 2000, Pan *et al* 2011), despite the diversity of loss and recovery pathways among degraded and secondary forest types (Poorter *et al* 2016).

Parallel ACD recovery curves in years 1–5 following logging and fire may reflect common site constraints, distinct mechanisms of forest growth, and model calibration. For example, different mechanisms of vegetation recovery and canopy closure may generate similar changes in estimated ACD, such as small gains in mean canopy height in logged forests and fast height growth of shorter resprouting or surviving trees in burned forests. Additionally, given that logging intensity is the single best predictor of ACD recovery time (Rutishauser *et al* 2015), evidence for greater extracted wood volume of low-value species in frontier forests (Richardson and Peres 2016) than in interior forests and experimental logging sites may explain differences with previous estimates of ACD recovery in logged forests (e.g. Chambers *et al* 2004, Putz *et al* 2012, Andrade *et al* 2017). Further, moisture availability is a critical constraint on regeneration rates (Poorter *et al* 2016, Wagner *et al* 2016); moisture stress from the seasonality of the study site may limit recovery rates in both logged and burned forests. Additional observations in repeatedly burned forests are needed to constrain long-term estimates of recovery patterns (>5 years) in the more heavily degraded sites.

Airborne lidar captures details about 3D forest structure needed to quantify aboveground carbon stocks and advance quantitative reporting on biodiversity safeguards and other co-benefits of REDD+. Individual tree and plot-level data from airborne lidar provide insights into the mechanisms driving biomass variability and habitat impacts from forest degradation. The residual density of large canopy trees, which can be directly quantified using high-density airborne lidar, is an important driver of ACD variability in degraded forests (Slik *et al* 2013), and closely corresponds to the spatial patterns of fire-induced canopy mortality (figure S7). In addition to ACD, the loss of canopy trees may also alter the forest micrometeorology, aerodynamic roughness, and successional success of grasses and lianas (Ray *et al* 2005, Silvério *et al* 2013). These changes, in turn, can increase vulnerability to windthrow and repeated fires, especially during drought years (e.g. Balch *et al* 2015). Canopy trees also serve as biodiversity refugia; the slower recovery of canopy tree clusters than carbon stocks in this study may suggest a more persistent impact of degradation on biodiversity than biomass in the first decades following logging or fire, consistent with findings from Martin *et al* (2013). Characterizing the time-integrated effects of avoided degradation on forest structure is clearly an important step for policies and management that aim to promote the retention of both biomass and biodiversity. Measurement and monitoring capabilities to support REDD+ commitments to safeguard biodiversity and promote other co-benefits are not yet operational (Goetz *et al* 2015). This work highlights the potential of airborne lidar to advance REDD+ MRV for both carbon and non-carbon objectives.

Our findings provide a detailed characterization of the carbon and habitat changes following Amazon forest degradation, but additional measurements are needed to assess regional variability in degradation impacts. Additional lidar samples across gradients in land use, forest type, and climate may identify important differences in degradation impacts and ACD recovery. For example, previous work suggests that transitional forests along the southern extent of the Amazon may be more resilient to mortality from a

single, low-severity fire during average weather conditions (Brando *et al* 2012) than interior forests. By contrast, forests in Central Amazon floodplains have exposed roots during dry periods, thin bark, and lack the ability to resprout, rendering them more vulnerable to fire-induced dieback (Flores *et al* 2017). Additionally, multi-temporal observations are needed to unequivocally attribute ACD losses to degradation, characterize delayed mortality, and investigate the potential for arrested succession (Barlow *et al* 2003). Multi-temporal studies may also help constrain interannual variability in fire damages (Brando *et al* 2014), consistent with the ~15% difference in ACD observed in this study between low and high-severity damages within a single fire. Complementary field measurements may help characterize key aspects of degraded forest structure that are not well captured by airborne lidar, such as the species distribution of regeneration from seeds or sprouts and the selective impact of degradation on mean wood density (Bunker *et al* 2005, Longo *et al* 2016). Lastly, the strong correspondence between changes in Landsat surface reflectance and lidar-derived estimates of forest structure and ACD in burned forests may support regional estimates of carbon losses from understory fires using Landsat or similar moderate resolution imagery.

## Conclusion

Forest degradation is ubiquitous in frontier Amazon forests, and damages from logging and fire were larger and longer lasting than previously reported for our southern Amazon study region. Combining the look-up table of emissions estimates from this study with activity data from satellite monitoring programs may allow for regional estimates of combined emissions from deforestation and forest degradation for REDD+. Understory fires—particularly, repeated burns—pose the greatest risk to forest carbon stocks and canopy structure along the Amazon arc of deforestation. Thus, avoiding additional fires in frontier landscapes may have an outsized benefit for carbon retention and habitat. Routine monitoring of frontier forests with airborne lidar may provide additional insights regarding the direct impacts of forest degradation on both carbon stocks and forest structure, including potential interannual variability from climate controls on fire severity or market influences on logging removals. Our approach to disentangle the complex legacy of degradation by combining forest inventory, airborne lidar, and Landsat time series offers a blueprint to generate degradation emissions factors in other geographies and regional circumstances.

## Acknowledgments

This work was partially supported by a National Science Foundation Doctoral Dissertation Research Improvement Grant (grant 1634168), a NASA Earth and Space Science Fellowship (D Rappaport), and NASA's Carbon Monitoring System program. Additional support was provided by the Brazilian National Council for Scientific and Technological Development (CNPq, grant 457927/2013-5) and Science Without Borders program (D Morton), and the São Paulo State Research Foundation (FAPESP, grant 2015/07227-6, M Longo). M Keller was supported as part of the Next Generation Ecosystem Experiments-Tropics, funded by the US Department of Energy, Office of Science, Office of Biological and Environmental Research. Support for data acquisition and M.N. dos-Santos was provided by the Sustainable Landscapes Brazil project, a collaboration of the Brazilian Agricultural Research Corporation (EMBRAPA), the US Forest Service, USAID, and the US Department of State. We gratefully acknowledge the assistance from Hyeungu Choi with lidar data processing.

## ORCID iDs

Danielle I Rappaport https://orcid.org/0000-0001-9122-9684
Douglas C Morton https://orcid.org/0000-0003-2226-1124
Marcos Longo https://orcid.org/0000-0001-5062-6245
Michael Keller https://orcid.org/0000-0002-0253-3359
Maiza Nara dos-Santos https://orcid.org/0000-0003-2720-2393

## References

Aguiar A P D *et al* 2016 Land use change emission scenarios: anticipating a forest transition process in the Brazilian Amazon *Glob. Change Biol.* **22** 1821–40

Alencar A, Nepstad D and Diaz M C V 2006 Forest understory fire in the Brazilian Amazon in ENSO and Non-ENSO years: area burned and committed carbon emissions *Earth Interact.* **10** 1–17

Andrade R B, Balch J K, Parsons A L, Armenteras D, Roman-Cuesta R M and Bulkan J 2017 Scenarios in tropical forest degradation: carbon stock trajectories for REDD+ *Carbon Balance Manage.* **12** 6

Aragão L E O C and Shimabukuro Y E 2010 The incidence of fire in Amazonian forests with implications for REDD *Science* **328** 1275–8

Aragão L E O C, Poulter B, Barlow J B, Anderson L O, Malhi Y, Saatchi S, Phillips O L and Gloor E 2014 Environmental change and the carbon balance of Amazonian forests *Biol. Rev.* **89** 913–31

Asner G P, Keller M, Pereira R Jr, Zweede J C and Silva J N 2004 Canopy damage and recovery after selective logging in Amazonia: field and satellite studies *Ecol. Appl.* **14** 280–98

Asner G P, Knapp D E, Broadbent E N, Oliveira P J, Keller M and Silva J N 2005 Selective logging in the Brazilian Amazon *Science* **310** 480–2

Avitabile V *et al* 2016 An integrated pan-tropical biomass map using multiple reference datasets *Glob. Change Biol.* **22** 1406–20

Baccini A et al 2012 Estimated carbon dioxide emissions from tropical deforestation improved by carbon-density maps *Nat. Clim. Change* **2** 182–5

Balch J K, Nepstad D C, Brando P M, Curran L M, Portela O, De CARVALHO O and Lefebvre P 2008 Negative fire feedback in a transitional forest of southeastern Amazonia *Glob. Change Biol.* **14** 2276–87

Balch J K et al 2015 The susceptibility of southeastern Amazon forests to fire insights from a large scale burn experiment *BioScience* **65** 893–905

Barlow J, Peres C A, Lagan B O and Haugaasen T 2003 Large tree mortality and the decline of forest biomass following Amazonian wildfires *Ecol. Lett.* **6** 6–8

Becknell J M, Kissing Kucek L and Powers L 2012 Aboveground biomass in mature and secondary seasonally dry tropical forests: a literature review and global synthesis *Forest Ecol. Manage.* **276** 88–95

Berenguer E, Ferreira J, Gardner T A, Aragão L E O C, De Camargo P B, Cerri C E, Durigan M, Oliveira R C D, Vieira I C G and Barlow J 2014 A large-scale field assessment of carbon stocks in human-modified tropical forests *Glob. Change Biol.* **20** 3713–26

Bergen K M, Goetz S J, Dubayah R O, Henebry G M, Hunsaker C T, Imhoff M L, Nelson R F, Parker G G and Radeloff V C 2009 Remote sensing of vegetation 3-D structure for biodiversity and habitat: Review and implications for lidar and radar spaceborne missions *J. Geophys. Res. Biogeosci.* **114**

Boisier J P, Ciais P, Ducharne A and Guimberteau M 2015 Projected strengthening of Amazonian dry season by constrained climate model simulations *Nat. Clim. Change* **5** 656–60

Brando P M, Nepstad D C, Balch J K, Bolker B, Christman M C, Coe M and Putz F E 2012 Fire-induced tree mortality in a neotropical forest: the roles of bark traits, tree size, wood density and fire behavior *Glob. Change Biol.* **18** 630–41

Brando P M et al 2014 Abrupt increases in Amazonian tree mortality due to drought–fire interactions *Proc. Natl Acad. Sci.* **111** 6347–52

Brazil 2014 Brazil's submission of a Forest Reference Emission Level (FREL) for reducing emissions from deforestation in the Amazonia biome for REDD+ results-based payments under the UNFCCC

Bunker D E, DeClerck F, Bradford J C, Colwell R K, Perfecto I, Phillips O L, Sankaran M and Naeem S 2005 Species loss and aboveground carbon storage in a tropical forest *Science* **310** 1029–31

Bustamante M et al 2016 Toward an integrated monitoring framework to assess the effects of tropical forest degradation and recovery on carbon stocks and biodiversity *Glob. Change Biol.* **22** 92–109

Canadell J G and Raupach M R 2008 Managing forests for climate change mitigation *Science* **320** 1456–7

Chambers J Q, Higuchi N, Teixeira L M, Dos Santos J, Laurance S G and Trumbore S E 2004 Response of tree biomass and wood litter to disturbance in a Central Amazon forest *Oecologia* **141** 596–611

Chen Y, Randerson J T, Morton D C, DeFries R S, Collatz G J, Kasibhatla P S, Giglio L, Jin Y and Marlier M E 2011 Forecasting fire season severity in South America using sea surface temperature anomalies *Science* **334** 787–91

Duffy P B, Brando P, Asner G P and Field C B 2015 Projections of future meteorological drought and wet periods in the Amazon *Proc. Natl Acad. Sci.* **112** 13172–7

Flores B M, Holmgren M, Xu C, van Nes E H, Jakovac C C, Mesquita R C G and Scheffer M 2017 Floodplains as an Achilles' heel of Amazonian forest resilience *Proc. Natl Acad. Sci.* **114** 4442–6

Friedlingstein P, Meinshausen M, Arora V K, Jones C D, Anav A, Liddicoat S K and Knutti R 2014 Uncertainties in CMIP5 climate projections due to carbon cycle feedbacks *J. Clim.* **27** 511–26

Gatti L V et al 2014 Drought sensitivity of Amazonian carbon balance revealed by atmospheric measurements *Nature* **506** 76–80

Goetz S J, Hansen M, Houghton R A, Walker W, Laporte N and Busch J 2015 Measurement and monitoring needs, capabilities and potential for addressing reduced emissions from deforestation and forest degradation under REDD+ *Environ. Res. Lett.* **10** 123001

Griscom B W et al 2017 Natural climate solutions *Proc. Natl Acad. Sci.* **114** 11645–50

Hansen A J, Phillips L B, Dubayah R, Goetz S and Hofton M 2014 Regional-scale application of lidar: variation in forest canopy structure across the southeastern US *Forest Ecol. Manage.* **329** 214–26

Holdsworth A R and Uhl C 1997 Fire in Amazonian selectively logged rain forest and the potential for fire reduction *Ecol. Appl.* **7** 713–25

Houghton R A, Skole D L, Nobre C A, Hackler J L, Lawrence K T and Chomentowski W H 2000 Annual fluxes of carbon from deforestation and regrowth in the Brazilian Amazon *Nature* **403** 301–4

INPE 2015 Amazon program - monitoring the Brazilian Amazon by satellite: the Prodes, Deter, Degrad and Terraclass systems (www.inpe.br)

Keller M, Asner G P, Silva J M N and Palace. M 2004 Sustainability of selective logging of upland forests in the Brazilian Amazon: carbon budgets and remote sensing as tools for evaluation of logging effects *Working Forests in the American Tropics: Conservation Through Sustainable Management?* ed D J Zarin, J Alavalapati, F E Putz and M Schmink (New York: Colombia University Press) pp 41–63

Le Page Y, Morton D, Hartin C, Bond-Lamberty B, Pereira J M C, Hurtt G and Asrar G 2017 Synergy between land use and climate change increases future fire risk in Amazon forests *Earth Syst. Dyn.* **8** 1237

Le Quéré C, Andrew R M, Canadell J G, Sitch S, Korsbakken J I, Peters G P, Manning A C, Boden T A, Tans P P and Houghton R A 2016 Global carbon budget 2016 *Earth Syst. Sci. Data* **8** 605

Longo M, Keller M M, dos-Santos M N, Leitold V, Pinagé E R, Baccini A, Saatchi S, Nogueira E M, Batistella M and Morton D C 2016 Aboveground biomass variability across intact and degraded forests in the Brazilian Amazon *Glob. Biogeochem. Cycles* **30** 1639–60

Martin P A, Newton A C and Bullock J M 2013 Carbon pools recover more quickly than plant biodiversity in tropical secondary forests *Proc. R. Soc.* B **280** 20132236

Matricardi E A T, Skole D L, Cochrane M A, Pedlowski M and Chomentowski W 2007 Multi-temporal assessment of selective logging in the Brazilian Amazon using Landsat data *Int. J. Remote Sens.* **28** 63–82

Mertz O et al 2012 The forgotten D: challenges of addressing forest degradation in complex mosaic landscapes under REDD+ Geografisk Tidsskrift-Danish *J. Geogr.* **112** 63–76

Morton D C, DeFries R S, Nagol J, Souza Jr. C M, Kasischke E S, Hurtt G C and Dubayah R 2011 Mapping canopy damage from understory fires in Amazon forests using annual time series of Landsat and MODIS data *Remote Sens. Environ.* **115** 1706–20

Morton D C, Page Y L, DeFries R, Collatz G J and Hurtt G C 2013 Understorey fire frequency and the fate of burned forests in southern Amazonia *Phil. Trans. R. Soc. B Biol. Sci.* **368** 20120163

Nobre C A, Sampaio G, Borma L S, Castilla-Rubio J C, Silva J S and Cardoso M 2016 Land-use and climate change risks in the Amazon and the need of a novel sustainable development paradigm *Proc. Natl Acad. Sci.* **113** 10759–68

Pan Y et al 2011 A large and persistent carbon sink in the world's forests *Science* **333** 988–93

Penman J *et al* 2003 *Good Practice Guidance for Land Use, Land-Use Change and Forestry* (Kanagawa: IPCC National Greenhouse Gas Inventories Programme, Institute for Global Environmental Strategies)

Pereira D, Santos D, Vedoveto M, Guimarães J and Veríssimo A 2010 *Fatos Florestais* (Imazon: Belém, PA)

Poorter L *et al* 2016 Biomass resilience of Neotropical secondary forests *Nature* **530** 211–4

Putz F E *et al* 2012 Sustaining conservation values in selectively logged tropical forests: the attained and the attainable *Conserv. Lett.* **5** 296–303

Ray D, Nepstad D and Moutinho P 2005 Micrometeorological and canopy controls of fire susceptibility in a forested Amazon landscape *Ecol. Appl.* **15** 1664–78

Richardson V A and Peres C A 2016 Temporal decay in timber species composition and value in Amazonian logging concessions *PLoS ONE* **11** e0159035

Rutishauser E *et al* 2015 Rapid tree carbon stock recovery in managed Amazonian forests *Curr. Biol.* **25** R787–8

Sato L Y, Gomes V C F, Shimabukuro Y E, Keller M, Arai E, dos-Santos M N, Brown I F and e Cruz de Aragão L E O 2016 Post-fire changes in forest biomass retrieved by airborne LiDAR in Amazonia *Remote Sens.* **8** 839

Slik J W F *et al* 2013 Large trees drive forest aboveground biomass variation in moist lowland forests across the tropics *Glob. Ecol. Biogeogr.* **22** 1261–71

Silva C A, Crookston N L, Hudak A T and Vierling L A 2015 rLiDAR: An R package for reading, processing and visualizing LiDAR (Light Detection and Ranging) data, version 0.1

Silvério D V, Brando P M, Balch J K, Putz F E, Nepstad D C, Oliveira-Santos C and Bustamante M M C 2013 Testing the Amazon savannization hypothesis: fire effects on invasion of a neotropical forest by native cerrado and exotic pasture grasses *Phil. Trans. R. Soc. B Biol. Sci.* **368** 20120427

Souza C M, Roberts D A and Monteiro A 2005 Multitemporal analysis of degraded forests in the southern Brazilian Amazon *Earth Interact.* **9** 1–25

Souza A P, Mota L L, Zamadei T, Martin C C, Almeida F T and Paulino J 2013 Classificação climática e balanço hídrico climatológico no estado de Mato Grosso *Nativa* **1** 34–43

Uhl C and Vieira I C G 1989 Ecological impacts of selective logging in the Brazilian Amazon: a case study from the Paragominas region of the state of Pará *Biotropica* 98–106

van der Werf G R, Morton D C, DeFries R S, Olivier J G, Kasibhatla P S, Jackson R B, Collatz G J and Randerson J T 2009 $CO_2$ emissions from forest loss *Nat. Geosci.* **2** 737–8

Vargas R, Allen M F and Allen E B 2008 Biomass and carbon accumulation in a fire chronosequence of a seasonally dry tropical forest *Glob. Change Biol.* **14** 109–24

Wagner F H *et al* 2016 Climate seasonality limits leaf carbon assimilation and wood productivity in tropical forests *Biogeosci. Katlenburg-Lindau* **13** 2537–62